MASTER

AEC RESEARCH AND DEVELOPMENT REPORT

HW-64286

THE H-1 HIGH TEMPERATURE GRAPHITE IRRADIATION EXPERIMENT

J. M. DAVIDSON and J. W. HELM

APRIL, 1961

HANFORD LABORATORIES

HANFORD ATOMIC PRODUCTS OPERATION
RICHLAND, WASHINGTON

GENERAL ELECTRIC

DISCLAIMER

This report was prepared as an account of work sponsored by an agency of the United States Government. Neither the United States Government nor any agency Thereof, nor any of their employees, makes any warranty, express or implied, or assumes any legal liability or responsibility for the accuracy, completeness, or usefulness of any information, apparatus, product, or process disclosed, or represents that its use would not infringe privately owned rights. Reference herein to any specific commercial product, process, or service by trade name, trademark, manufacturer, or otherwise does not necessarily constitute or imply its endorsement, recommendation, or favoring by the United States Government or any agency thereof. The views and opinions of authors expressed herein do not necessarily state or reflect those of the United States Government or any agency thereof.

DISCLAIMER

Portions of this document may be illegible in electronic image products. Images are produced from the best available original document.

LEGAL NOTICE

This report was prepared as an account of Government sponsored work. Neither the United States, nor the Commission, nor any person acting on behalf of the Commission:

A. Makes any warranty or representation, expressed or implied, with respect to the accuracy, completeness, or usefulness of the information contained in this report, or that the use of any information, apparatus, method, or process disclosed in this report may not infringe privately owned rights; or

B. Assumes any liabilities with respect to the use of, or for damages resulting from the use of any information, apparatus, method, or process disclosed in this report.

As used in the above, "person acting on behalf of the Commission" includes any employee or contractor of the Commission, or employee of such contractor, to the extent that such employee or contractor of the Commission, or employee of such contractor prepares, disseminates, or provides access to, any information pursuant to his employment or contract with the Commission, or his employment with such contractor.

AEC-GE RICHLAND, WASH.

HW-64286

UC-40, Radiation Effects on
Materials
(TID-4500, 16th Ed.)

THE H-1 HIGH TEMPERATURE GRAPHITE IRRADIATION EXPERIMENT

By

J. M. Davidson and J. W. Helm

Materials Development
Reactor and Fuels Research and Development
Hanford Laboratories Operation

April, 1961

HANFORD ATOMIC PRODUCTS OPERATION
RICHLAND, WASHINGTON

Work performed under Contract No. AT(45-1)-1350 between
the Atomic Energy Commission and General Electric Company

Printed by/for the U. S. Atomic Energy Commission

Printed in USA. Price $1.25. Available from the
Office of Technical Services
Department of Commerce
Washington 25, D. C.

TABLE OF CONTENTS

THE H-1 HIGH TEMPERATURE GRAPHITE IRRADIATION EXPERIMENT

INTRODUCTION

Knowledge of the effect, rate, and magnitude of radiation-induced contraction of graphite in its physical dimensions is important to designers and operators of graphite-moderated reactors. For example, contraction of graphite can lead to distortion of process channels in horizontally tubed reactors which use graphite for structural support. Also, differential radiation-induced contraction caused by flux and temperature gradients through large graphite bars, under certain circumstances, may cause stresses leading to fracture.

Because some types of reactors are susceptible to these serious problems resulting from contraction, more extensive information concerning this important radiation damage effect was sought early through the use of high flux irradiation facilities. Implementing this study, the H-1 Experiment in the General Electric Test Reactor (GETR) compared contraction behavior of a selected series of graphites and, in particular, behavior at temperatures in excess of 750 C, which is an area of knowledge heretofore incomplete and speculative. The graphites selected for testing were those that appeared to meet the contemporary theoretical criteria for stability under irradiation to long exposures at high temperatures. The capsule was designed for and operated at temperatures of 800-1200 C in a flux of 3.2×10^{14} nv, $E > 0.18$ Mev.

In the H-1 Experiment, gamma heating was used to achieve the desired irradiation temperatures, since self-heated capsules are feasible in reactors having high gamma-heating rates if an appropriate heat transfer design is utilized. The validity of using only gamma heating in conjunction with appropriate heat leakage to obtain desired test conditions in graphite irradiations was demonstrated in the GEH-13 Experiments performed in the Engineering Test Reactor (ETR) core. Desired irradiation temperatures could have been

achieved also with a combination of gamma and electrical heating, but the omission of heaters and auxiliary equipment made possible simultaneous irradiation of a larger number of samples. At the time of the H-1 Experiment, a large number of untested but promising graphites were available, thus favoring the choice of a gamma-heated, large inventory capsule.

SUMMARY

A high temperature graphite irradiation experiment was performed in the GETR core to determine the effects of differences in manufacturing, formulation and graphitization temperatures on radiation-induced contraction. The experiment was performed at temperatures of 800-1200 C in an intense fast neutron flux. The maximum integrated exposure of the sample positions was 3.2×10^{21} nvt, E > 0.18 Mev, corresponding to approximately 24,000 MWD/AT in a conventional graphite-moderated reactor.

All the graphites tested, with the exception of the controls, were needle coke filler, coal tar pitch binder graphites varying in particle size, graphitization temperature and impregnation. From theoretical and experimental considerations, the formulations and treatments were expected to result in a relatively stable graphite in the direction transverse to extrusion. For comparison of the experimental results to existing experience, a conventional graphite, CSF, was used at each irradiation position. The results showed that the graphite most stable to contraction was graphitized at a high temperature (> 3100 C) and made from small particle size (all flour) filler. In all cases, the needle coke graphite contracted at a lower rate than the CSF graphite. Differences attributable to the size of extrusion and/or post graphitization cooling rate were discerned readily.

Auxiliary to the purposes of the experiment, the apparent thermal neutron cross section for Co^{58} (plus Co^{58m}) was determined. Co^{58} and Co^{58m} are the products of the Ni^{58} (n, p) reaction, which is used widely for fast flux monitoring. Both have large thermal neutron capture cross sections which must be accounted for to prevent error in fast neutron dosimetry. In this experiment, a value was determined for the apparent burn-out cross section of 3750 barns.

DESIGN AND CONSTRUCTION OF EXPERIMENT

The desired operating temperature of the H-1 Experiment was achieved by balancing the gamma heating of the capsule against the designed heat losses to the reactor coolant. Sample sizes and mounting configurations were considered analytically until the desired heat transfer characteristics were obtained. At operating temperatures of the H-1 Experiment, a large part of the heat transfer is by radiation. This allows greater confidence in design because radiative transfer is exponential and tends to stabilize temperatures despite normal variations in gamma-heating rate. At lower temperatures where conductive modes prevail, the uncertainty in thermal conductivity concomitant with the linear temperature response of conductive transfer limits the predictability and stability of the temperature at which the samples operate. The design and heat transfer calculations of the finished capsule are shown in Appendix I.

The H-1 Experiment was designed functionally to irradiate eight types of graphite represented by 48 samples. The samples are described by parameters of manufacture and by vendor in Appendix II. For comparison, these samples were arranged in two groups based on initial bar size: Group I contained CSF, GL-10, GL-11, and VC; and Group II included RC, RX-1, RX-2, and RX-3. Group I samples were from four-inch square extrusions manufactured in graphite production plants; Group II samples were from two-inch diameter round extrusions manufactured in the National Carbon Company Research Laboratory in research furnaces. The VC and RC types of graphite are equivalent except as described above. The use of the two-inch diameter extrusions was necessary to obtain, in a short time, graphite which varied by type of coke, temperature, particle size, and impregnation. The direction tested was transverse to the graphite extrusion axis in each case.

The samples were machined in quarter-round shapes two inches long and then were heated to 1300 C to relieve a small, thermally annealable strain invariably present in graphite.[1] The variable expansion resulting from heating is only about 0.02 per cent, but it is large enough to interfere with the accuracy of contraction measurements. A cylindrical subassembly

of four quarter-round samples of Group I was joined with a graphite ring to a like subassembly of Group II samples. The assemblies were mounted in the capsule in a manner to provide alternation of the sample groups. In this way, each extrusion size was tested in the full range of temperature and exposure with uniform experimental conditions at each position within a group. The alternation also served as a safeguard against gross experimental failure if samples in one or several positions in the experiment failed. The CSF samples were included for comparison with previous experience.

An internal view of the capsule is illustrated in Figure 1. The sample groups were held mechanically by insulating holders inserted in transverse molybdenum disks attached to cooling rings. The disks, 0.005 inch thick, served as a thermal barrier, prevented lateral motion of the holders and samples, and allowed longitudinal motion due to thermal expansion. The cooling rings were connected by aluminum spacing tubes which were fitted on aluminum pins screwed into the rings. Also attached to the cooling rings were small cans holding flux monitors. The cooling rings, while serving a structural purpose, held the thermocouples in place and prevented them from melting by providing a thermal sink. After the assembled samples and related structure were inserted in the outer shell, the capsule was sealed by welding the upper and lower caps. A lead tube, which provided a watertight egress for the thermocouple leads, penetrated the upper cap. The lead tube terminated in a watertight gland. The lower cap had an evacuation tube for helium filling and leak testing. The protective cap for the evacuation tube was designed additionally to restrict the reactor coolant flow in the annular region between the capsule and the lower part of the capsule guide tube.

An exploded view of the lead termination seal is shown in Figure 2. The lead tube from the experiment was welded to the seal housing. The primary seal was made with a Conax gland. The thermocouple lead wires ran through holes in a Hanford-made polyethylene packing plug which provided a seal when compressed in the Conax gland by porcelain insulators. Although polyethylene is mechanically inferior to the usual neoprene or Teflon sealant, its radiation resistance is substantially better. The wires penetrating the

AEC-GE WASH.

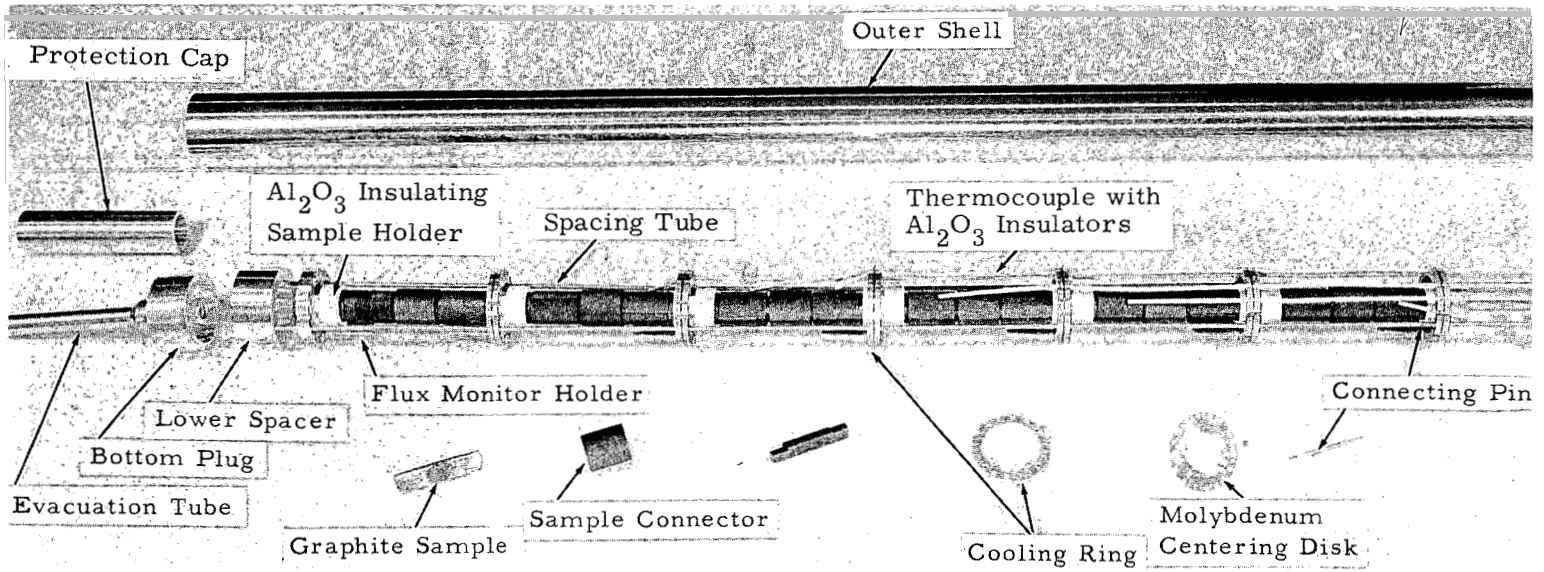

FIGURE 1

H-1 Capsule During Construction

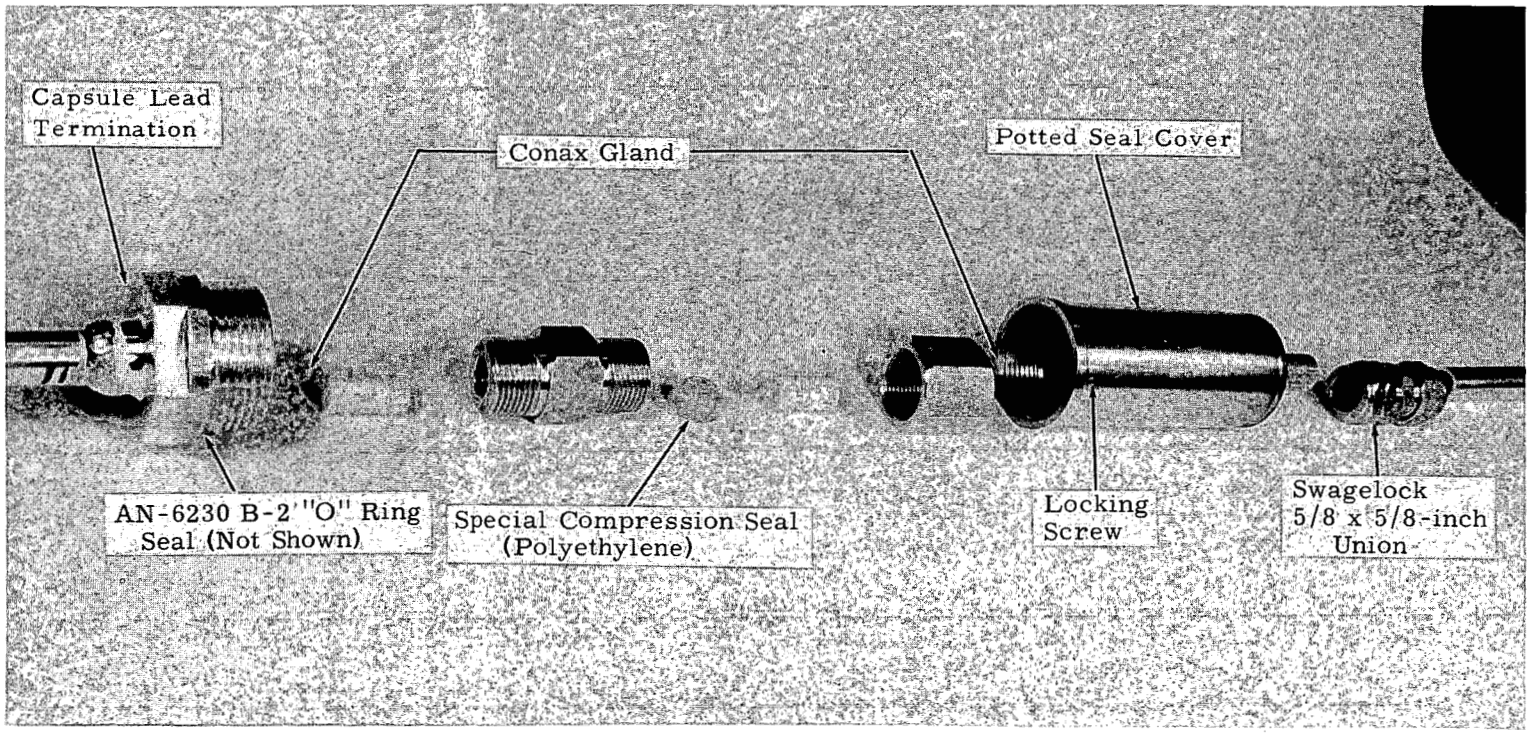

FIGURE 2

Lead Seal (Exploded View)

This seal provides the primary water seal to the capsule lead. It is located in the reactor tank and prevents water from reaching the capsule in the event of a leak in the secondary piping.

Conax gland were attached to secondary lead wires. The seal cover acted as a secondary protective seal. The exterior surfaces of the gland and the interior surface of the seal cover were treated with Dow-Corning Primer No. A-4094. The cap then was filled with General Electric silicone rubber No. RTV-60, after which the seal cover was attached and locked by set screws to prevent turning. The tubing end of the cap allowed mechanical attachment of a secondary lead tube, which carried the leads from the seal to the reactor access flange through a GETR funnel tube.

Prior to filling with helium, the capsule and upper seal were tested at 65 psig with nitrogen introduced in the evacuation tube at the lower end. While under pressure, the capsule was tested for large leaks with soap solution. After the capsule passed the soap test, it was evacuated and filled with helium to a pressure of 780 mm of mercury. The slight excess pressure prevented contamination of the gas during closure and allowed testing of the final closure by helium leak detection. The evacuation tube then was crimped shut at two places, separated by 0.5 inch. At the outermost crimp, the evacuation tube was cut off and welded. The weld and other seals were checked again for leaks. The protective cap of the evacuation tube was attached and locked with set screws.

EXPERIMENTAL PROCEDURE

Installation

The H-1 Experiment first was installed in the GETR in August, 1959. During the initial increase in water flow, the lead bracket failed from severe vibration and the lead fractured. The experiment was removed from the GETR and, because no new graphite stock was available, the samples were salvaged for reconstruction of a new capsule before the next shutdown. The samples were removed, dried, and heated to 1300 C. After new length measurements, they were installed in a new capsule made from spare parts. The second capsule was installed in September, 1959. At that time, the lead tube was braced more substantially, and the experiment operated thereafter without incident. A schematic plan and elevation view of the installation

are in Figure 3. In this installation, the lead tube and seal were contained in a two-inch diameter, Schedule-40 aluminum pipe with the E-5 filler piece as an integral part of the lower end. The upper end of the guide tube was held in the loop support bracket which traverses the pressure vessel immediately below the top flange. Two centering rings were placed on the lead tube to prevent vibration of the tube within the pipe. From the top seal, the lead tube was run inside a reactor funnel tube, then through the outlet flange to a seal pot.

Temperature Instrumentation

At installation, seven of eight chromel-alumel thermocouples operated. The temperatures were measured and recorded as long as the thermocouples remained operable. Although it was expected that the thermocouples would fail prior to the completion of the test, records of temperature stability until failure were kept to allow estimates of the temperature during the entire irradiation. During the first irradiation cycle, a thermocouple operating at 800 C failed. After two cycles of irradiation, the remaining thermocouples were erratic in output and later became electrically open. In general, the temperatures observed during irradiation agreed with the calculations made prior to installation.

Post-Irradiation Disassembly

After 75.6 effective days at full reactor power, the capsule was discharged in January, 1960, and was removed to the Radioactive Materials Laboratory at Vallecitos, where it was disassembled.

In the disassembly procedure, the capsule ends were cut off with a tube cutter and the can was slit longitudinally in two cuts 180 degrees apart with a high speed, air-driven abrasive wheel. When the capsule was opened, it showed some internal damage from the irradiation. Figure 4 shows the condition of the capsule immediately after opening. A considerable sooty deposit, in excess of the quantity expected, was spread throughout the capsule. Its distribution indicates that the material was carried to the wall by gas convection. There is little doubt that the graphite samples were the source

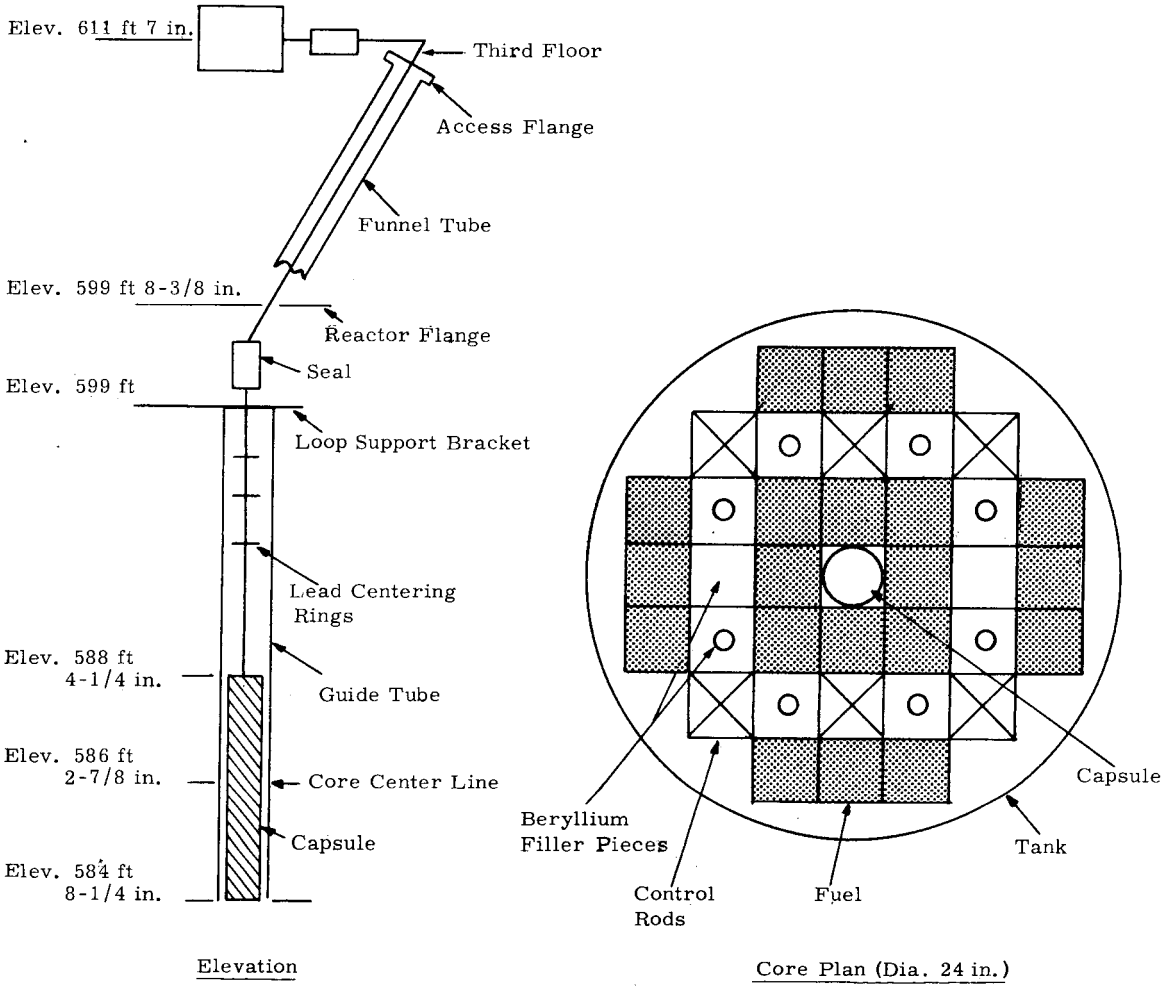

FIGURE 3

Schematic Diagram of Experiment Installation

AEC-GE RICHLAND, WASH.

AEC-GE RICHLAND, WASH.

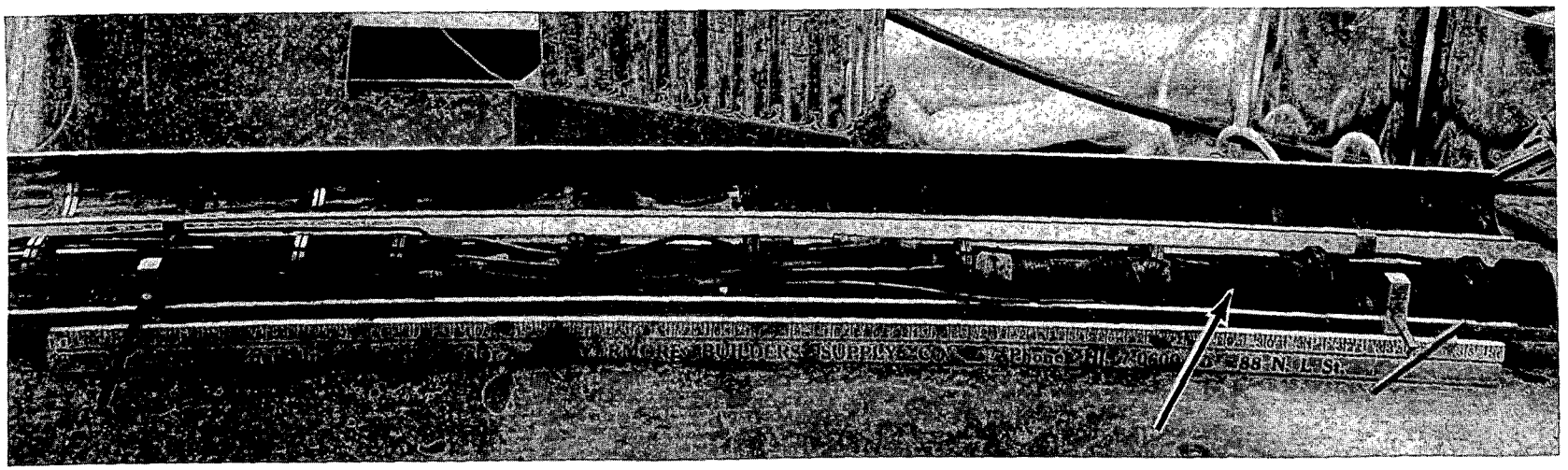

FIGURE 4

H-1 Capsule After Irradiation

The deposits on the can wall are graphite.
Some sample displacement was caused during disassembly.
Arrow indicates melted spacing rod.

of the deposit: first, because some of the material was identified crystallographically as graphite; and second, because of the absence of any other carbonaceous substances in the capsule as fabricated. The mechanism of graphite erosion is not understood presently. Two aluminum spacing rods in the highest gamma-heating zone melted partially and some of the insulating holders were burned slightly. The thermocouples were intact and showed no evidence of melting. This evidence limits the upper temperature of the samples to less than 1500 C, a fact corroborated by the thermocouple readings prior to failure. It was not possible to determine how the thermocouples failed.

Sample Measurement

Measurements of length were made optically and physically on all samples prior to irradiation. A Bausch & Lomb DR-25 Optical Gage (Type 33-14-23) was used for physical end-to-end measurements, and a Bausch & Lomb Bench Comparator (Type 33-12-11) for measurements of the distances between spaced holes drilled in the samples. These devices, when used for measurement of graphite, have a standard deviation of replication of 5×10^{-5} and 16×10^{-5} inches, respectively.

The post-irradiation condition of some samples is shown in Figures 5 and 6. The photographs compare samples from a typical zone and from the most highly damaged zone of the capsule. In cases of the samples with damaged ends, optical hole-to-hole measurements of length were used. In other cases, the optical measurements were used only to substantiate the more reproducible end-to-end measurements.

Determination of Exposure

Theoretical and experimental techniques were used to determine the exposure of the H-1 Experiment. The integrated flux above 0.18 Mev was of principal interest, but to describe completely the conditions of exposure, the thermal and resonance fluxes also were determined. At the inception of the experiment, it was intended to rely on foil dosimetry for estimation of the exposure; however, small post-irradiation differences between theoretical and

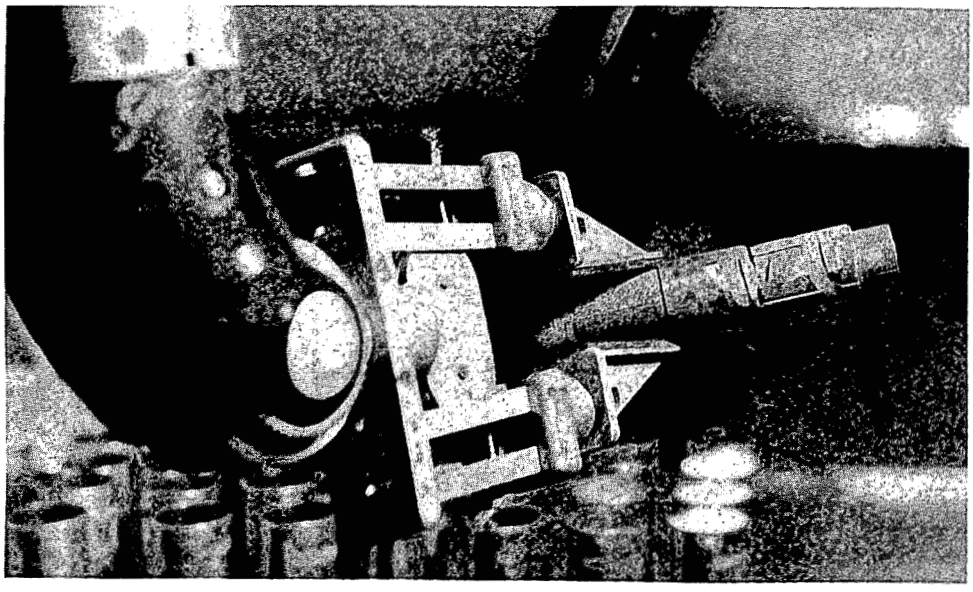

FIGURE 5

Sample Subassembly from Typical Position

The scraping marks are from scuffing by the molybdenum disk (axial constraint). The sample ends are in good condition.

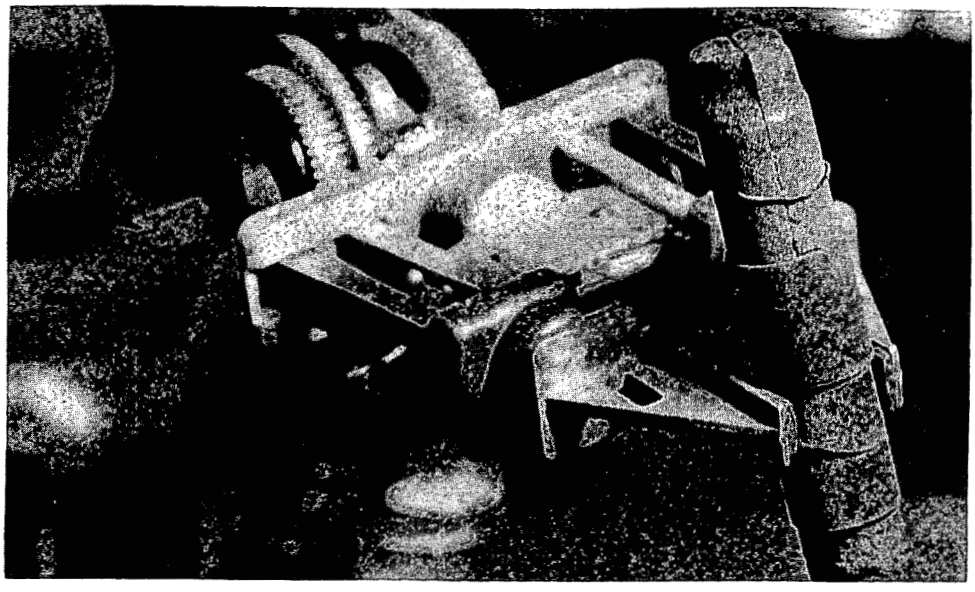

FIGURE 6

Sample Subassembly from Highly Damaged Position

The end damage resulted from reaction with impurities in the cement used in construction of sample holders.
End measurements could not be made on these samples.

AEC-GE RICHLAND, WASH.

experimental estimates of fast flux necessitated arbitrary selection of one technique for data reduction purposes. The theoretically derived fluxes have been used in this report.

The thermal flux monitors were 0.1 per cent cobalt-aluminum alloy in the form of 0.020 inch diameter wire, and some cadmium-covered thermal wires were included to determine the resonance flux. Nickel foils were installed for fast flux monitoring, utilizing the high energy (n, p) reaction leading to $Co^{58} + Co^{58m}$. Cobalt-58 ($T_{1/2}$ = 72 days), formed both directly and through the decay of the short-lived metastable Co^{58m}, is measured readily from a relatively sharp 0.82-Mev gamma emission. Although nickel has been used extensively and recommended as a flux monitor,[2] the large thermal neutron cross sections for the Co^{58} products were discovered only recently. A recent value cited is 1500 barns;[3] however, in a reactor flux of high intensity, the apparent cross section may be as large as 3500 barns.[4] This cross section is based on irradiations of nickel in the MTR and ETR. The varying cross sections at different intensities may be due to preferential interaction of neutrons during irradiation with the short-lived, metastable Co^{58m} isomer, believed to have a cross section in excess of 150,000 barns. An average apparent Co^{58} thermal cross section of 3750 barns was necessary for agreement between cadmium-protected nickel foils and bare nickel foils irradiated by the authors in the GETR F-3 position as an adjunct to the H-3 Experiment (Appendix III). Thus, for the conditions of this experiment, the feasibility of using nickel solely as an integrating fast monitor is impaired because of thermal neutron intensity dependence.

Theoretical calculations of the flux were made with an IBM 704 digital computer using a PDQ code.[5] Three neutron energy groups were calculated at each of 5884 mesh points taken over one-half the core area. These were φ_1 (>0.18 Mev), φ_2 (0.17 ev-0.18 Mev), and φ_3 (<0.17 ev). Calculations were performed for three of the four cycles of the irradiation and are shown in Table I.

TABLE I

E-5 AVERAGE FLUX

Cycle	$\varphi_1 \times 10^{-14}$	$\varphi_2 \times 10^{-14}$	$\varphi_3 \times 10^{-14}$
5	3.10	2.80	1.60
6	3.24	2.92	1.76
7*	3.24	2.92	1.76
8	3.41	2.79	1.80
Average	3.25	2.86	1.73

* Not calculated, core same as Cycle 6.

The flux values cited were the average flux intensities for the spatial-material composition representing the H-1 capsule, filler block, and water at the point of average axial intensity. The intensities of several mesh points chosen radially in the capsule did not differ significantly from the composition average.

Irradiation facilities in the GETR penetrate the core vertically. The calculations mentioned previously give the neutron flux at the vertical point of average intensity; thus, it was necessary to determine the axial (or longitudinal) flux distribution. This was accomplished experimentally. For thermal neutrons, the peak-to-average ratio in the E-5 position was fixed at 1.55 by the use of cobalt wires. The fast neutron axial distribution, while resembling the thermal distribution, was somewhat different. To determine the fast distribution, nickel wire shielded with 0.040 inch thick cadmium tubes was irradiated in a nearby position, F-3, during Cycle 15, a short cycle. Measurement was made with shielded nickel during a short operating cycle instead of at the beginning of a cycle at low power, thereby obtaining an average full power flux distribution. Moreover, a short cycle would not burn out the cadmium covers, an inevitable problem in high flux multicycle irradiations. The experimentally derived flux distribution resulting from the calibrating irradiation is shown

in Figure 7. With knowledge of the longitudinal variation of fast flux and the PDQ calculated average flux for the E-5 position, the exposures for all positions of the H-1 capsule were calculated.

While it is premature to consider quantitative variations in fast flux spectra in reckoning radiation damage, it seemed desirable to compute the fast neutron spectrum for future evaluation of the irradiation results. The neutron spectrum between 0.18 Mev and 10 Mev was determined with high resolution by the use of a modified GNU-II calculation.[6] The neutron density determined in this calculation for each of twenty intervals in the range 0.18 Mev to 10 Mev normalized to an intergral value of one is shown in Figure 8.

IRRADIATION RESULTS

The restriction of the H-1 Experiment to a comparison of contractions in different types of graphite was imposed by insufficient knowledge of the convertability of GETR irradiation to other irradiation experiences. Presently, little is known about the dependence of graphite contraction at high temperatures on the intensity of the fast flux. Some preliminary results by Yoshikawa of current investigations at low temperatures show little, if any, dependence on intensity.[7] The effect of spectral differences at high energies is also of concern and little understood. This, too, is being studied.[8] Between light water-moderated and graphite-moderated reactors there is little difference in spectra above 2 Mev, but differences in the moderation of high energy neutrons cause a substantial difference in spectra below 2 Mev.

One of the particular problems of the H-1 Experiment was the inter-dependent nature of neutron flux intensity and gamma heating; this resulted in exposure and temperature of irradition being proportional. Since other irradiation data[9] indicate an approximately linear relationship between exposure and contraction (after a small initial expansion) to exposures of 10,000 MWD/AT, application of that relationship to the data from this experiment seems justified. Thus, contraction rates were considered to be independent of exposure and affected only by temperature.

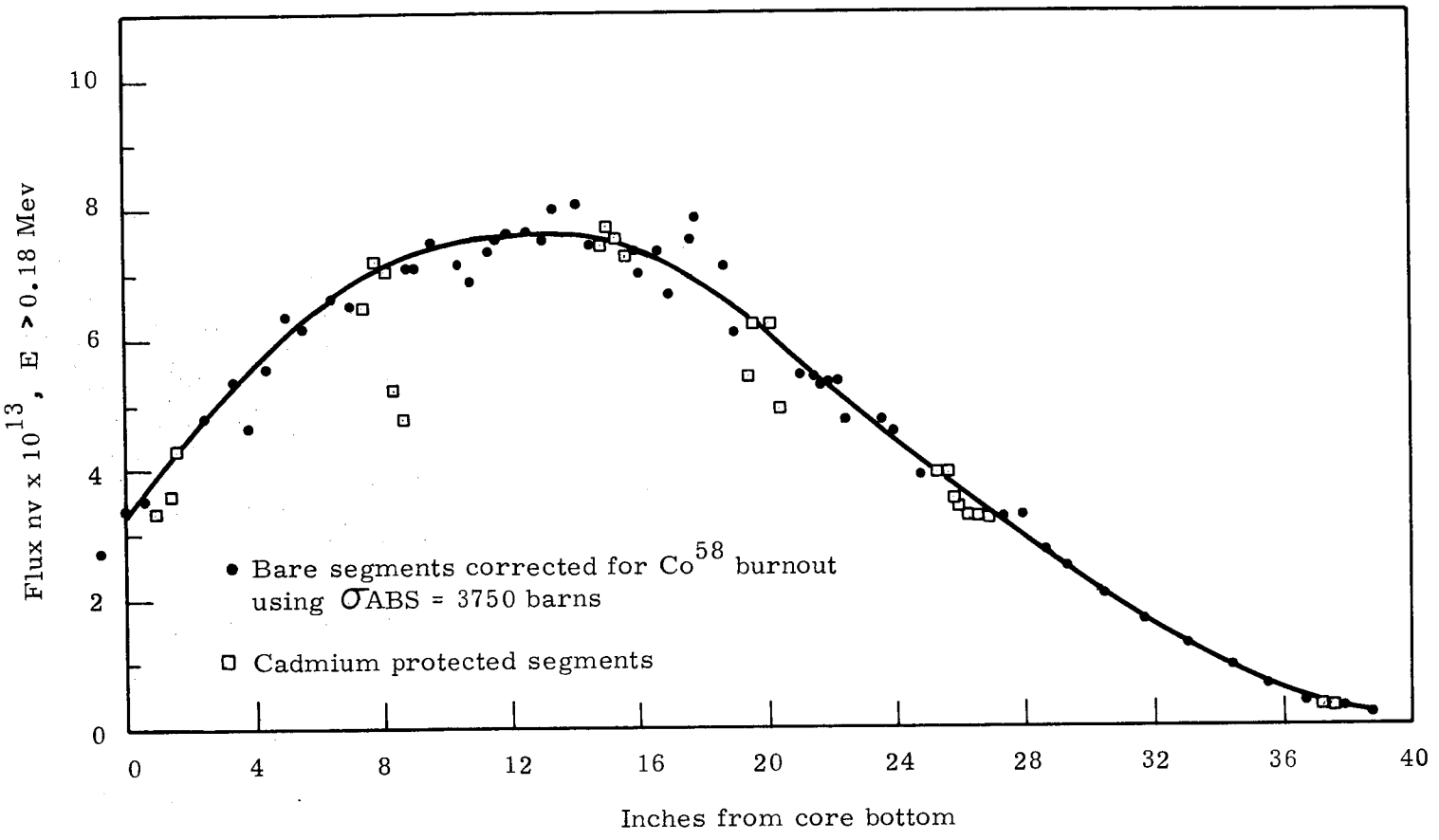

FIGURE 7

Fast Flux Distribution in F-3

Results are from a nickel wire irradiated during Cycle 15.

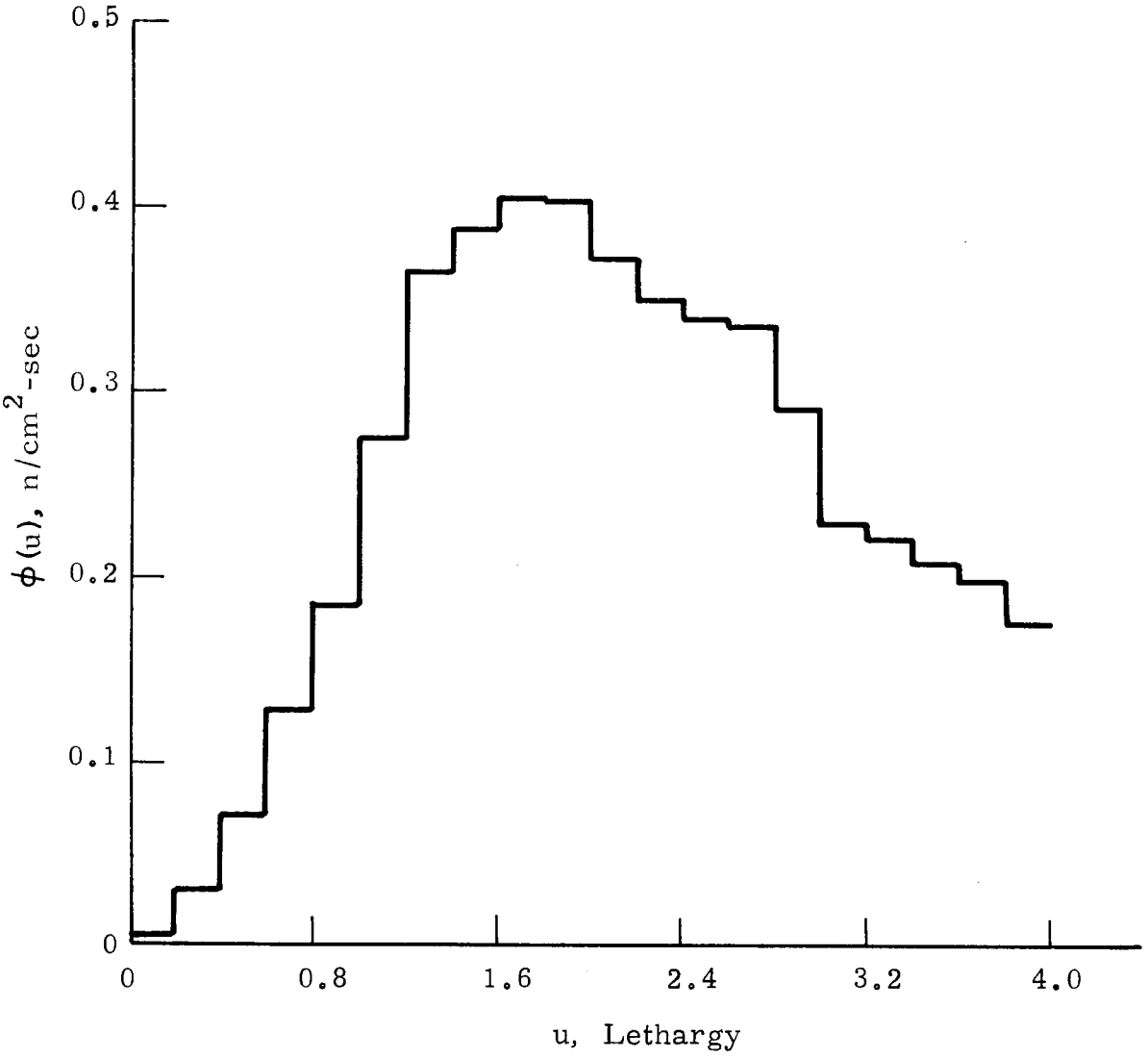

FIGURE 8

Neutron Spectral Distribution in E-5

The integral between lethargy 0 and 4 has been normalized to one neutron per cm^2 per second.

AEC-GE RICHLAND, WASH.

The results from irradiation are shown in Table II, along with the experimental parameters of temperature and exposure. From the different behavior at positions of comparable conditions of the VC and RC samples which, except for extrusion size and post-graphitization cooling rates, were the same, an adjustment seems necessary to compare data from the two-inch round extrusions with data from four-inch square extrusions. Only within each group can valid comparisons of manufacturing processes be obtained.

In the two-inch extrusion size, RC is the most similar to VC, which was the least contracting of the four-inch extursions. Among the two-inch extrusions, RC displayed the greatest contraction and RX-3 the least. Therefore, it is concluded that the least contracting material would be a graphite produced in a four-inch extrusion, but otherwise using the manufacturing process which produced RX-3 with the possible exception of the post-graphitization cooling rate used for the two-inch extrusion. RX-3 was an all-flour, Continental coke graphite which was graphitized at 3140 C, the highest graphitization temperature for any graphite in this test (Appendix II).

The improvement of needle coke graphites over CSF diminishes at high temperatures, but in all cases they are measurably better. If it is assumed that contraction is a linear function of the exposure, the data can be normalized to a selected exposure, and rates of contraction can be derived as a function of temperature. Figures 9 and 10 show the results of this treatment with normalization to 10^{21} nvt, E>0.18 Mev.

Changes of the crystallite parameters, $\underline{c}$ (twice the interplanar distance) and L_c (the crystallite size perpendicular to the planes), due to irradiation were measured and are shown in Tables III and IV.

The changes in $\underline{c}$ are small and somewhat random, although all changes show some expansion of the lattice. Changes in the crystallite size, L_c, appear sensitive to temperatures up to approximately 900 C and thereafter depend principally on exposure.

TABLE II

SUMMARY OF LENGTH CHANGES, PER CENT Δ L/L ± 0.01

		Graphite Type							
	Exposure	Group I				Group II			
Temp. C	10^{-21} nvt, E > 0.18 Mev	CSF	GL-10	GL-11	VC	RC	RX-1	RX-2	RX-3
800	1.3	-0.05	-0.03	-0.04	-0.03				
850	1.6					-0.10	-0.05	-0.06	-0.04
950	2.0	-0.06	-0.02	-0.06	-0.03				
1000	2.4					-0.16	-0.08	-0.08	-0.07
1100	2.8	-0.14	-0.12	-0.14	-0.10				
1150	3.1					-0.31	-0.26	-0.34	-0.21
1200	3.2	-0.35	-0.24	-0.29	-0.22				
1200	3.2					-0.45	-0.37	-0.37	-0.20
1150	3.2	-0.29	-0.22	-0.26	-0.05				
1100	3.0					-0.43	-0.32	-0.37	-0.27
1050	2.7	-0.13	-0.12	-0.13	-0.06				
1000	2.2					-0.15	-0.12	-0.16	-0.11

AEC-GE RICHLAND, WASH.

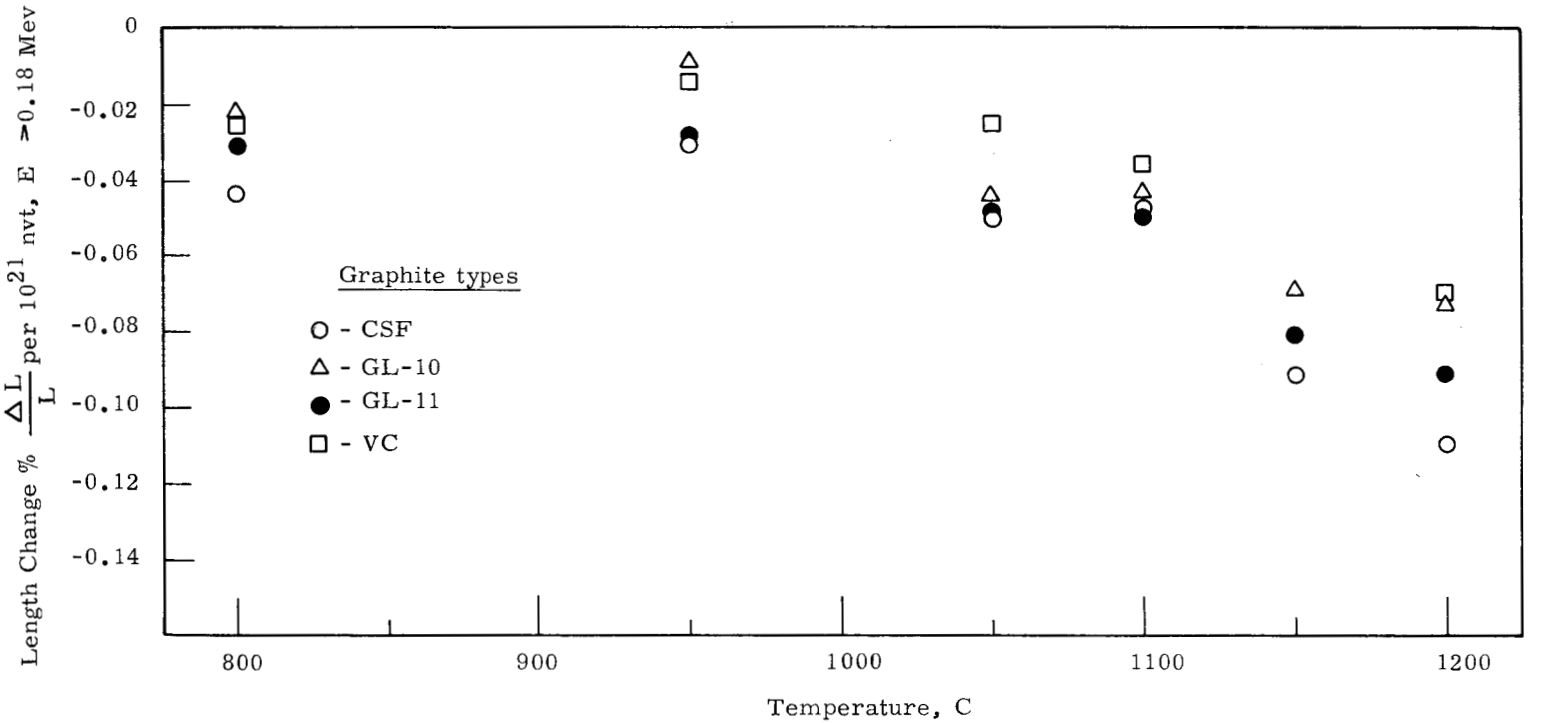

FIGURE 9

Contraction Behavior of Group I Graphites as a Function of Temperature

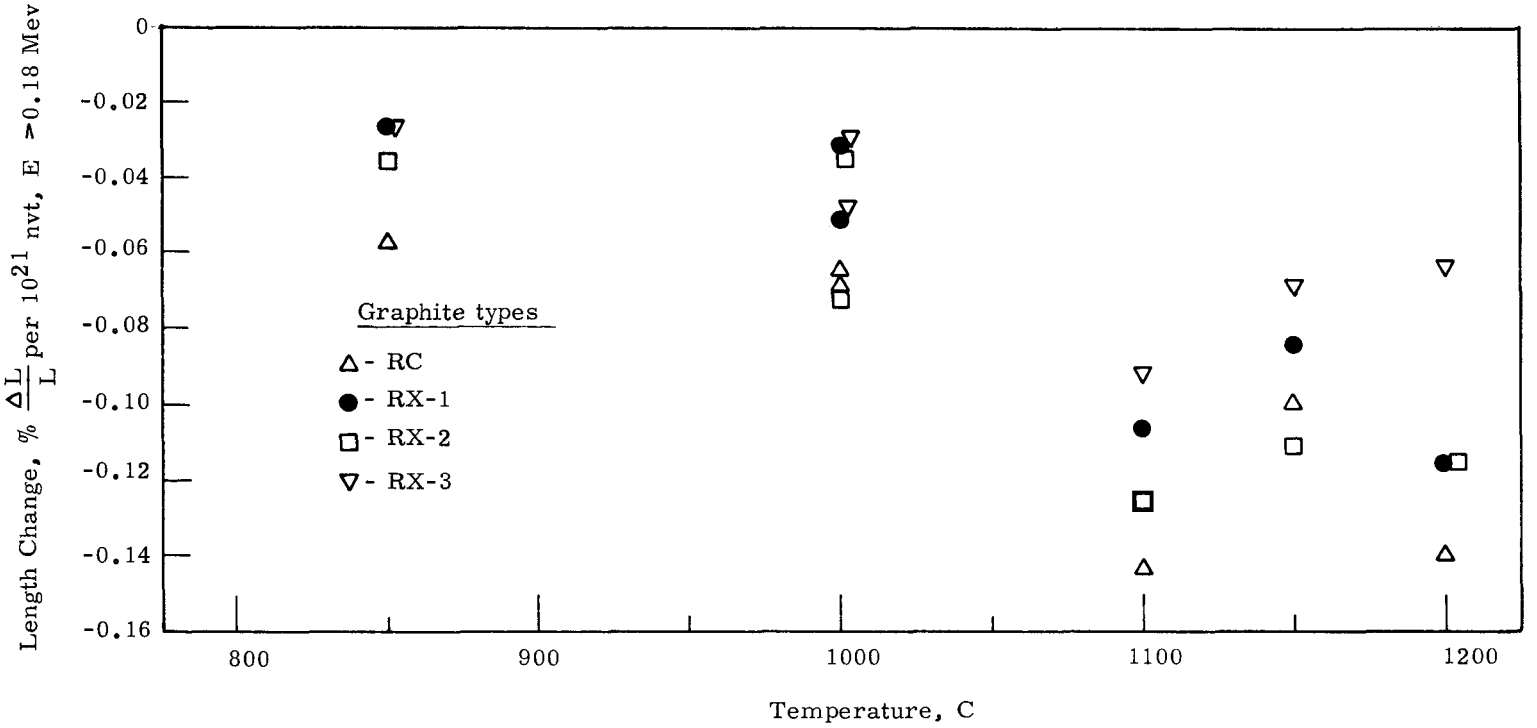

FIGURE 10

Contraction Behavior of Group II Graphites as a Function of Temperature

TABLE III

INITIAL VALUES AND CHANGES IN c (Å)

Temp., C	Exposure 10^{-21} nvt, E > 0.18 Mev	Graphite Type: Group I CSF	GL-10	GL-11	VC	Group II RC	RX-1	RX-2	RX-3
800	1.3	6.709 +0.025	6.719 +0.016	6.712 +0.029	6.702 +0.030				
850	1.6					6.698 +0.031	6.720 +0.026	6.717 +0.022	6.708 +0.019
950	2.0	6.705 +0.022	6.709 +0.018	6.727 +0.005	6.702 +0.030				
1000	2.4					6.698 +0.034	6.712 +0.032	6.717 +0.022	6.695 +0.032
1100	2.8	6.709 +0.016	6.719 +0.006	6.712 +0.017	6.702 +0.027				
1150	3.1					6.698 +0.057	6.705 +0.009	6.717 - 0.005	6.708 +0.009
1200	3.2	6.720 0	6.719 - 0.004	6.712 +0.015	6.702 +0.015				
1200	3.2					6.698 +0.031	6.712 +0.005	6.717 - 0.012	6.721 - 0.004
1150	3.2	6.702 +0.019	6.729 - 0.010	6.696 +0.016	6.702 +0.005				
1100	3.0					6.698 +0.028	6.712 +0.017	6.717 - 0.005	6.708 +0.013
1050	2.7	6.709 +0.023	6.719 +0.010	6.712 +0.013	6.702 +0.027				
1000	2.2					6.698 +0.023	6.712 +0.015	6.717 - 0.003	6.708 +0.013

TABLE IV

INITIAL VALUES AND CHANGES IN L_c (Å)

Temp., C	Exposure 10^{-21} nvt, E >0.18 Mev	Graphite Type: Group I CSF	GL-10	GL1-11	VC	Group II RC	RX-1	RX-2	RX-3
800	1.3	760	700	560	740				
		-355	-395	-255	-345				
850	1.6					550	700	710	770
						-175	-415	-370	-400
950	2.0	760	700	535	740				
		-455	-355	-235	-371				
1000	2.4					550	590	790	745
						-252	-315	-547	-475
1100	2.8	760	700	560	740				
		-517	-430	-328	-497				
1150	3.1					550	480	710	770
						-373	-277	-495	-575
1200	3.2	760	700	495	740				
		-579	-517	-330	-562				
1200	3.2					550	590	630	800
						-395	-408	-457	-625
1150	3.2	760	700	640	740				
		-598	-535	-299	-551				
1100	3.0					550	590	710	770
						-382	-409	-515	-572
1050	2.7	760	700	560	740				
		-582	-485	-345	-557				
1000	2.2					550	590	710	770
						-285	-325	-435	-440

APPENDIX I

DESIGN AND HEAT TRANSFER CALCULATIONS

SUMMARY

FLUX MAXIMUM VALUES (Design)	
Neutron, nv:	
10-0.18 Mev	3.2×10^{14}
0.18 Mev-0.17 ev	2.6×10^{14}
Less than 0.17 ev	1.4×10^{14}
Gamma Heating, watts/g:	16
Btu/(hr)(g):	54.7
SAMPLE DESCRIPTION	
Assembly Size:	
Graphite Cylinder	4.25 inches long 13/16 inches in diameter
Weight:	
Sample, g	54.2
Assembly, g/ft	483
HEAT GENERATION	
Graphite Core, Btu/(hr)(ft):	11,000
Total Assembly, Btu/(hr)(ft):	26,400
MAXIMUM HEAT FLUX, Btu/(hr)(sq ft)	50,200
COOLANT CONDITIONS	
Water Flow Past Capsule, gpm:	100
Water Velocity Past Capsule, ft/sec:	8
TEMPERATURES	
Capsule Surface Temperature, F:	145
Sample Temperature Range, F:	1840-2580
Sample Temperature Range, C:	1000-1420
GAS ATMOSPHERE	
Helium Pressure, psia at 1500 C:	90
MECHANICAL STRENGTH, SAFETY FACTOR	
Collapsing:	6.0

A. CAPSULE TEMPERATURES AND HEAT FLUX

Calculation of the Maximum Can Wall Temperature

1. Coolant Conditions

Water Flow	100 gpm
Velocity Past Capsule	8 ft/sec
Equivalent Diameter	D_e = 0.223 in. = 0.0186 ft

2. Data for Water at 120 F (Ref. 10)

Density, ρ	61.7 lb/cu ft
Viscosity, μ	1.36 lb/(hr)(ft)
Thermal Conductivity, k	0.372 Btu/(hr)(sq ft)(°F/ft)
Heat Capacity, c	1.0 Btu/(lb)(°F)

3. Water Film Coefficient, h

$$h = 0.020 \frac{k}{D} (N_{RE})^{0.8} (N_{PR})^{0.33} \quad \text{(Ref. 11)}$$

Reynolds Number N_{RE}

$$N_{RE} = \frac{D_e V \rho}{\mu}$$

$$= \frac{0.0186 \text{ ft} \times 8 \text{ ft/sec} \times 61.7 \text{ lb/cu ft} \times 3600 \text{ sec/hr}}{1.36 \text{ lb/(hr)(ft)}}$$

$$= 2.43 \times 10^4$$

Prandtl Number, N_{PR}

$$N_{PR} = \frac{c \mu}{k}$$

$$= \frac{1.0 \text{ Btu/(lb)(°F)} \times 1.36 \text{ lb/(hr)(ft)}}{0.372 \text{ Btu/(hr)(sq ft)(°F/ft)}}$$

$$= 3.65$$

$$h = 0.020 \frac{k}{D} (2.43 \times 10^4)^{0.8} (3.65)^{0.33}$$

$$= \frac{0.372 \text{ Btu/(hr)(sq ft)(°F/ft)}}{0.0186 \text{ ft}} [0.020 (0.323 \times 10^4)(1.54)]$$

$$= 1990 \text{ Btu/(hr)(sq ft)(°F)}$$

Therefore the water film coefficient is 1990 Btu/(hr)(sq ft)(°F).

4. Heat Generation, q

Basis

Sample Length, Inches	2
Sample Assembly Length, Inches	4.25
Maximum Flux, Btu/(hr)(g)	54.6

Mass

	Assembly (grams)	Core (grams)
Graphite Samples	54.2	54.2
Alundum Support	16.8	16.8
Aluminum Spacer + Flux Monitor Can	20.7	--
Aluminum Can - 4.25-Inch Section	79.5	--
Total, 4.25-Inch Section	171.2	71.0
Per Foot	483.0	200.0

Assembly Core, q_c = 200 g/ft x 54.6 Btu/(hr)(g) = 11,000 Btu/(hr)(ft)

Assembly Section, q_a = 483 g/ft x 54.6 Btu/(hr)(g) = 26,400 Btu/(hr)(ft)

5. Heat Flux, Assembly

$$\frac{q}{A} = 50,200 \text{ Btu/(hr)(sq ft)}$$

6. Film Temperature Drop

$$\Delta T = \frac{q/A}{h}$$

$$= \frac{50,200 \text{ Btu/(hr)(sq ft)}}{1990 \text{ Btu/(hr)(sq ft)(°F)}}$$

$$= 25.3 \text{ F}$$

7. Internal Can Wall Temperature

Temperature Drop Across Can Wall

$$\Delta t = \frac{q \ln D_2/D_1}{k\, 2\pi L}$$

For a 4.25-Inch Assembly Section

$$\Delta t = \frac{26,400 \text{ Btu/(hr)(ft)} \times 4.25/12 \text{ ft} \times \ln 2.00/1.87}{128 \text{ Btu/(hr)(ft)(°F)} \times 2\pi \times 4.25/12 \text{ ft}}$$

$$= 2 \text{ F}$$

Therefore, the maximum internal can wall temperature is 120 F + 25 F + 2 F = 147 F.

Calculation of the Sample Surface Temperature

1. Basic Data

Thermal Conductivities		Btu/(hr)(sq ft)(°F/ft)	
Graphite	212 F	60.5	(Ref. 12)
	1800 F	24.2	(Ref. 12)
Aluminum		128	(Ref. 12)
Alundum		0.97	(Ref. 13)
Vitreous Alumina		9.67	(Ref. 13)
Molybdenum		72	(Ref. 12)
Helium	200 F	0.0980	(Ref. 12)
	500 F	0.112	
	1000 F	0.133	
	1500 F	0.155	
	2000 F	0.172	
	2500 F	0.182	

Emissivities		ϵ	
Aluminum	200 F	0.20	(Ref. 10)
Alundum	1800 F	0.40	(Ref. 10)
Graphite	1800 F	0.80	(Ref. 10)

Aluminum Can	2 in. OD x 1.87 in. ID
Alundum Supports	1.062 in. OD x 0.750 in. ID x 1 in.
Aluminum Supports	1.86 in. OD x 1.375 in. ID x 0.313 in. thick
Molybdenum	1.375 in. effective OD x 1.031 in. effective ID x 0.005 in. thick

Gamma Flux

Peak Midplane, 16 watts/gram

For Design, Peak-to-Average Ratio of 1.78

F = 9.0 watts/gram

Sample Sizes

Assembly

Two 13/16 in. x 2 in. Subassemblies with 1 in. Graphite Connector - Total, 3-1/4 in.

With Alundum Holder, 4-1/4 in.

2. Thermal Resistance Calculation

Total resistance to heat flow, R_T, is formed by parallel combination of the following heat paths:

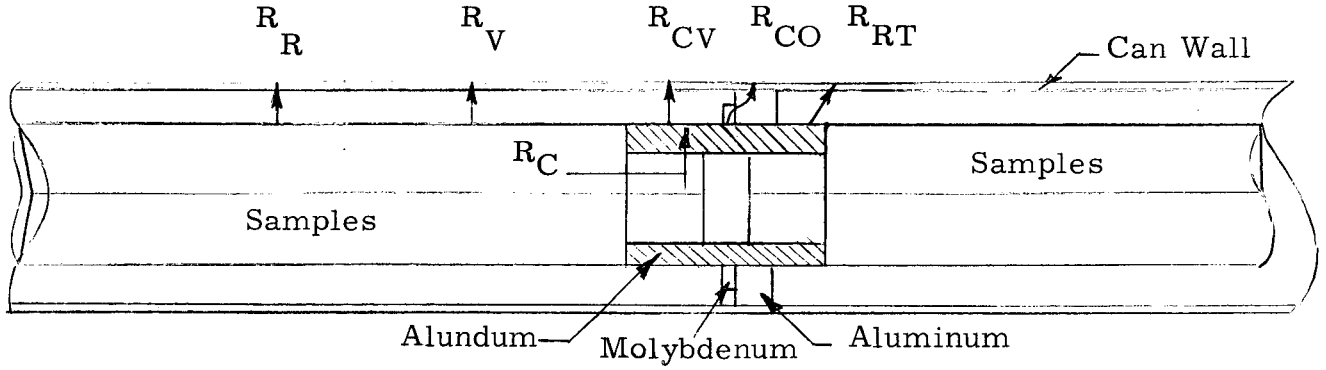

There are three parallel paths from samples to can wall:

R_R = radiation resistance,

R_V = resistance to conduction through helium, and

R_C = resistance to conduction through alundum supports.

There are three parallel paths from alundum to can wall:

R_{RT} = radiation resistance,
R_{CV} = resistance to conduction through helium, and
R_{CO} = resistance to conduction through molybdenum and aluminum supports.

Total resistance of alundum to can wall = R_{AC},

$$R_{AC} = \frac{1}{\frac{1}{R_{RT}} + \frac{1}{R_{CV}} + \frac{1}{R_{CO}}} .$$

The series path from sample to can wall through supports is

$$R_D = R_{AC} + R_C .$$

Total resistance, R_T, is

$$R_T = \frac{1}{\frac{1}{R_R} + \frac{1}{R_V} + \frac{1}{R_D}} .$$

Radiation Resistance

Sample to can wall, R_R

$$\mathcal{F}_{12} = \frac{1}{\frac{1}{\overline{F}} + (\frac{1}{\epsilon_1} - 1) + \frac{A_1}{A_2} (\frac{1}{\epsilon_2} - 1)}$$

$\overline{F}$ = 1 for coaxial cylinders

$$\mathcal{F}_{12} = \frac{1}{\frac{1}{1} + (\frac{1}{0.80} - 1) + \frac{0.813}{1.87} (\frac{1}{0.20} - 1)} = 0.334$$

$$h_r = \frac{4 \times 0.173 \times 0.334}{100} \left(\frac{T_{avg}}{100}\right)^3$$

$$= 0.00231 \left(\frac{T_{avg}}{100}\right)^3$$

$$R_R = \frac{1}{h_r A}$$

$$A = \frac{3.25 \times 0.813\ \pi}{12 \times 12} = 0.0576 \text{ sq ft}$$

$$R_R = \frac{1}{0.00231 \times 0.0576 \left(\frac{T_{avg}}{100}\right)^3} = \frac{7500}{\left(\frac{T_{avg}}{100}\right)^3}$$

Alundum to can wall, R_{RT}

$$\mathcal{F}_{12} = \frac{1}{\frac{1}{1} + \left(\frac{1}{0.40} - 1\right) + \frac{1.063}{1.87}\left(\frac{1}{0.20} - 1\right)} = 0.209$$

$$h_e = \frac{4 \times 0.173 \times 0.209}{100}\left(\frac{T_{avg}}{100}\right)^3 = 0.00144\left(\frac{T_{avg}}{100}\right)^3$$

$$A = \frac{1 \times 1.063\ \pi}{12 \times 12} = 0.0232 \text{ sq ft}$$

$$R_{RT} = \frac{}{0.0232 \times 0.00144\left(\frac{T_{avg}}{100}\right)^3} = \frac{29,800}{\left(\frac{T_{avg}}{100}\right)^3}$$

Resistance of Supports

Through alundum, R_C

$$R = \frac{\ln D_2/D_1}{2\ \pi L k}$$

$$R_C = \frac{\ln \frac{1.063}{0.75}}{2\ \pi(1/12)\ 0.967} = 0.689\ (°F)(hr)/Btu$$

Through molybdenum and aluminum, R_{CO}

$$R_M = 2\ \frac{\ln \frac{1.375}{1.831}}{2\ \pi \times \frac{0.005}{12} \times 72} = 3.06\ (°F)(hr)/Btu$$

(Only half of surface in contact)

$$R_{AL} = \frac{\ln \frac{1.86}{1.375}}{2\pi\left(\frac{0.313}{12}\right) 128} = 0.014\ (°F)(hr)/Btu$$

$$R_{CO} = R_M + R_{AL} = 3.07\ (°F)(hr)/Btu$$

$$\frac{1}{R_{CO}} = 0.326\ Btu/(hr)(°F)$$

Resistance of Gas

$$N_{GR} = \frac{x^3 \rho^2 g \beta \Delta t}{\mu^2}$$

$$x^3 = \left(\frac{D_2 - D_1}{2}\right)^3 = \left(\frac{1.87 - 0.812}{2}\right)^3 = 6.4 \times 10^{-5}\ \text{cu ft}$$

At 1000 F,

$$\rho^2 = (0.0114)^2 = 1.58 \times 10^{-4}\ (\text{lb/cu ft})^2$$

$$g = 4.19 \times 10^8\ \text{ft/hr}^2$$

$$\beta = \frac{1}{T_{avg}}\ °R = 1022\ R$$

$$\Delta t = 875\ F$$

$$\mu^2 = (0.0726)^2 = 5.3 \times 10^{-3}\ \left|\text{lb/(hr)(ft)}\right|^2$$

$$N_{Gr} = \frac{6.4 \times 10^{-5}\ \text{cu ft} \times 1.58 \times 10^{-4} (\text{lb/cu ft})^2 \times 4.19 \times 10^8\ \text{ft/hr}^2 \times 875\ °F}{1022\ °R \times 5.3 \times 10^{-3}\ \text{lb}^2 . \left|\text{lb/(hr)(ft)}\right|^2}$$

$$= 6.8 \times 10^3$$

or $N_{GR} < 2 \times 10^3$, therefore convection is suppressed, and conduction controls.

$$h_c = \frac{k}{x}$$

$$R = \frac{1}{h_c A} = \frac{\ln D_2/D_1}{2 k \pi L}$$

From samples to wall, R_V

$$R_V = \frac{\ln \frac{1.87}{0.813}}{2 k \pi \frac{3.25}{12}} = \frac{0.489}{k}$$

From alundum to wall, R_{CV}

$$R_{CV} = \frac{\ln \frac{1.87}{1.063}}{2 \pi k \frac{1}{12}} = \frac{1.08}{k}$$

Total Resistance, R_T, is summarized in Table V. The data are plotted in Figure 11.

3. Maximum Surface Temperature

Heat Input

Q_1 = 16 watts/gram x 71.0 grams x 3.42 Btu/(hr) per watt
= 3890 Btu/hr

Trial Temperature, 2550 F

T_1 = 2550 F T = 2550 - 147 = 2403 F

R_T = 0.62 F hr/Btu from Figure 11

$$Q_2 = \frac{2403 \text{ F}}{0.62 \text{ F/(hr)(Btu)}} = 3880 \text{ Btu/hr}$$

which satisfies the conditions that $Q_1 = Q_2$ at the temperature that produces a net resistance of the value calculated.

TABLE V

TOTAL RESISTANCE, R_T^*

T_1 °F	$\frac{1}{R_{RT}}$	$\frac{1}{R_{CO}}$	$\frac{1}{R_{CV}}$	$\frac{1}{R_{AC}}$	R_{AC}	R_C	R_D	$\frac{1}{R_D}$	$\frac{1}{R_R}$	$\frac{1}{R_V}$	$\frac{1}{R_T}$	R_T
200	0.0084	0.326	0.091	0.425	2.35	0.69	3.04	0.329	0.033	0.200	0.562	1.78
500	0.0160	0.326	0.104	0.446	2.24	0.69	2.93	0.342	0.063	0.229	0.634	1.58
1000	0.0368	0.326	0.123	0.486	2.06	0.69	2.75	0.364	0.146	0.272	0.782	1.28
1500	0.0704	0.326	0.143	0.539	1.86	0.69	2.55	0.392	0.280	0.316	0.988	1.01
2000	0.120	0.326	0.159	0.605	1.65	0.69	2.34	0.427	0.479	0.352	1.258	0.79
2500	0.190	0.326	0.169	0.685	1.46	0.69	2.15	0.465	0.755	0.372	1.592	0.63

* Data plotted on Figure 11.

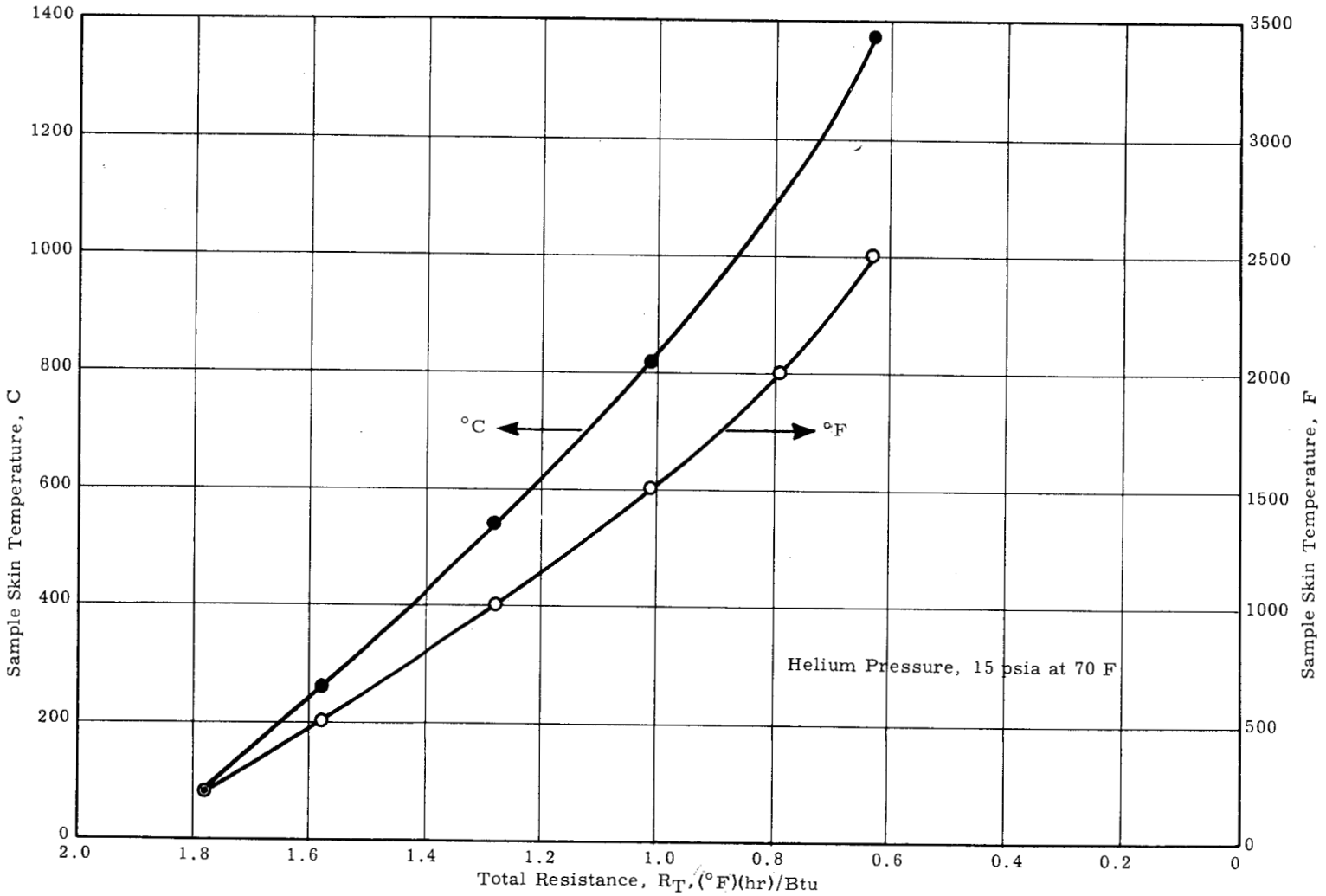

FIGURE 11

Thermal Resistance As a Function of Temperature

4. Minimum Surface Temperature

Heat Input

$$Q = 8 \text{ watts/gram} \times 71.0 \times 3.42 = 1945 \text{ Btu/hr}$$

Trial Temperature, 1825 F

$$T_2 = 1825 \text{ F} \quad T = 1825 - 147 = 1678 \text{ F}$$

$$R_T = 0.86 \text{ (°F)(hr)/Btu from Figure 11}$$

$$Q = \frac{1678}{0.86} = 1950 \text{ Btu/hr}$$

which satisfies the minimum heat flux condition.

Calculation of Maximum Sample Temperature

1. Temperature Drop in Graphite

$$\Delta T = \frac{r\,q'}{2AK}$$

$$= \frac{13/32 \text{ in.} \times 3890 \text{ Btu/hr} \times 54.2/71.0 \times 12 \text{ in./ft}}{2 \times \pi \times 13/16 \text{ in.} \times 4.25 \text{ in.} \times 24.2 \text{ Btu/(hr)(ft)(°F)}} = 27 \text{ F}$$

2. Maximum Temperature

$$2550 \text{ F} + 27 \text{ F} = 2577 \text{ F} = 1420 \text{ C}$$

Calculation of Minimum Sample Temperature

1. Temperature Drop in Graphite

$$\Delta T = \frac{13/32 \times 1945 \times 54.2/71.0 \times 12}{2 \times \pi \times 13/16 \times 4.25 \times 24.2} = 14 \text{ F}$$

2. Minimum Temperature

$$1825 \text{ F} + 14 \text{ F} = 1839 \text{ F} \cong 1000 \text{ C}$$

B. MECHANICAL STRENGTH

Collapsing Pressure, Ignoring the Support of the Cooling Rings

Can 2 in. OD x 0.065-in. wall

Material: 3003-H14 aluminum

Minimum Mechanical Properties

Yield Strength - compression 15,000 psi

Rating for Temperature, YS

100 per cent at 75 F

89 per cent at 212 F

$$P = 2 S_c \left[\frac{t}{D} - \left(\frac{t}{D}\right)^2\right]$$

$$P = 2(15,000 \times 0.89)(0.0325 - [0.0325]^2)$$

$$= 840 \text{ psia}$$

Reactor pressure 140 psia

Safety factor $\frac{840}{140} = 6.0$

APPENDIX II

GRAPHITE NOMENCLATURE

Hanford Designation	Supplier	Coke Source	Size, Inches	Remarks
		Conventional Coke Material		
CSF BAAD	National Carbon Co.	Cleves	4 x 4 x 50	Reactor grade, graphitized at 2700 C and F-purified. Density, 1.66 g/cc.
		Needle Coke Material		
GL-10 AAAD	Great Lakes Carbon Corporation	Proprietary Information	4 x 4 x 50	Great Lakes nuclear grade HPJ, thermally purified. Density, 1.60 g/cc. Graphitized at ~ 2800 C.
GL-11 AAAD	Great Lakes Carbon Corporation	Continential	4 x 4 x 50	Great Lakes nuclear grade HPDA, thermally purified. Density, 1.57-1.59 g/cc. Graphitized at ~ 2800 C.
VC AAAD	National Carbon Co.	Continential	4 x 4 x 50	AGOT processed. Regular particle size mix, one impregnation. Refinery process altered to produce Kendall-type coke. Density, 1.71 g/cc. Graphitized at ~ 2800 C.

GRAPHITE NOMENCLATURE (contd.)

Hanford Designation	Supplier	Coke Source	Size	Remarks
RC AAAD	National Carbon Co.	Continental	2-in. dia. x 8	Same as VC except processed in development laboratory. Density, 1.59 g/cc. Graphitized at ~2800 C. Cooled generally faster than graphite made in production furnaces.
RX-1 AAAD	National Carbon Co.	Continental	2-in. dia. x 8	Same as RC but fine mix, unimpregnated and graphitized at 2900 C. Density, 1.62 g/cc.
RX-2 AAAD	National Carbon Co.	Continental	2-in. dia. x 8	Same as RX-1 but impregnated. Density, 1.63 g/cc.
RX-3 AAAD	National Carbon Co.	Continental	2-in. dia. x 8	Same as RX-2 but graphitized at 3140 C. Density, 1.59 g/cc.

APPENDIX III

MEASUREMENT OF LONGITUDINAL FLUX DISTRIBUTION

To determine experimentally the longitudinal fast flux distribution, a 24-gage nickel wire, full core length, was irradiated in F-3 during Cycle 15. For uncompensated measurement of fast flux, sections of the wire were protected with cadmium covers to eliminate thermal neutron burnout of Co^{58} and Co^{58m}. This technique also allowed the calculation of the thermal neutron burn-out cross section for the combined products, termed here as apparent absorption cross section of Co^{58}. The calculation does not distinguish the relative burn-out rates in the Co^{58} and Co^{58m} branching. Due to the ratio of the cross sections of the metastable and ground states of Co^{58}, it is likely that the apparent cross section is intensity dependent for thermal flux intensities differing greatly from those observed in this experiment. The cadmium covers were made from sections of tubing one inch long with a 0.040-inch wall, and were spaced along the wire at six-inch intervals. After irradiation, the covers were removed, the entire wire cut into 1/4-inch segments, and the activities determined. The 0.82-Mev characteristic γ-emission was counted using a 256-channel analyzer.[16]

The governing equation for the rate of change of Co^{58} atoms is

$$\frac{dn}{dt} = \sigma_{act} N\varphi_f - \lambda n - \sigma_{abs} n \varphi_{th},$$

where:

n = number of Co^{58} atoms per milligram of foil,
N = number of Ni^{58} atoms per milligram of foil,
t = time,
σ_{act} = activation cross section for Ni^{58}
φ_f = average fast flux,
λ = disintegration constant for Co^{58}
σ_{abs} = apparent absorption cross section for Co^{58}, and
φ_{th} = average thermal flux.

Assuming φ_f to be a square wave, equal to a constant during each operating period and equal to zero during the shut-down periods, the following is obtained:

$$\varphi_f t_{op} = \frac{A}{\lambda \sigma_{act} N} \left[(\lambda + \sigma_{abs} \varphi_{th}) t_{op}\right] \left[\sum_{j=1}^{m} \frac{\left[1 - e^{-(\lambda + \sigma_{abs} \varphi_{th}) t_{ji}}\right]}{\left(e^{\lambda t_{js}}\right)\left(e^{(\lambda + \sigma_{abs} \varphi_{th}) t_{ji}} + 1\right) \cdots \left(e^{\lambda t_o}\right)}\right]^{-1} \quad (1)$$

where:

A = specific activity at time of counting of foil,

$t_{op} = \left[\sum_{j=1}^{m} t_{ji}\right]$ = the total operating time,

j = 1, 2, ... m = each operating time,

t_{ji} = operating time for the j^{th} operating period,

t_{js} = time of the shutdown following the j^{th} operating period,

t_o = time from the end of the last operating period to the date of foil counting,

λ = 9.62×10^{-3} day^{-1} or 1.114×10^{-7} sec^{-1},

N = 6.94×10^{18} mg^{-1}, and

σ_{act} = 120 mb (GETR spectrum E > 1 Mev).

For single cycle irradiations, Equation (1) with appropriate constants becomes

$$\varphi_f t_{op} (E > 1 \text{ Mev}) = \frac{1.07 \times 10^{-13} A(9.62 \times 10^{-13} + 8.64 \times 10^{-20} \sigma_{abs} \varphi_{th}) t_{op}}{\left[\frac{1 - e^{-\left(9.62 \times 10^{-3} + 8.64 \times 10^{-20} \sigma_{abs} \varphi_{th}\right) t_{op}}}{e^{(9.62 \times 10^{-3}) t_o}}\right]}, \quad (2)$$

with t in days and A in dis/(sec)(mg).

Longitudinal Flux Distribution

Use of Equation (1) requires the prior knowledge of the apparent absorption cross section of Co^{58} to calculate exposure from unprotected foil segments. Since the value was not known independently, the longitudinal distribution in F-3 was calculated from the activities of the protected segments. Using foil parameters of t_{op} = 12.6 days and t_o = 104.9 days and dropping the φ_{th} terms, Equation (2) becomes

$$\varphi_f t_{op} = 3.12 \times 10^{13} A,$$

which was used to compute the longitudinal distribution. The results are shown in Figure 7 and in Table VI.

Determination of σ_{abs}, the Apparent Thermal Burnout Cross Section

From the distribution obtained with the protected foils and knowledge of thermal flux, it is possible to solve Equation (2) for the apparent absorption cross section of Co^{58}. Letting $X = 9.62 \times 10^{-3} + 8.64 \times 10^{-20} \sigma_{abs} \varphi_{th}$, Table VI can be compiled. The solution, σ_{abs}, is in the column on the right.

The average burn-out cross section determined from the data in Table VI was 3741 barns (σ_m = 17). Taking the average value as 3750 barns, Equation (2) can be reapplied to give the exposures of the unprotected segments plotted in Figure 7.

TABLE VI

F-3 FOIL RESULTS

Wire Position, Inches from Core Bottom	Exposure, (E >1 Mev) nvt x 10^{-19} Cadmium-Shielded	dis/(sec)(mg) Bare Wire x 10^{-6}	$\frac{X}{1 - e^{-X}}$	X	φ_{th} nv x 10^{-14}	Apparent Co^{58} Absorption Cross Section σ_{abs}
0	3.60	0.908	0.1043	0.0456	1.09	3800
2	4.91	1.16	0.1120	0.0585	1.51	3753
4	6.08	1.39	0.1154	0.0638	1.68	3724
6	7.11	1.56	0.1206	0.0717	1.87	3827
8	7.78	1.63	0.1260	0.0798	2.18	3723
10	8.15	1.64	0.1311	0.0875	2.45	3670
12	8.31	1.65	0.1331	0.0905	2.52	3706
14	8.28	1.64	0.1334	0.0909	2.48	3794
16	8.02	1.62	0.1305	0.0866	2.33	3821
18	7.52	1.57	0.1260	0.0798	2.14	3783
20	6.66	1.44	0.1217	0.0733	1.99	3697
22	5.61	1.23	0.1203	0.0712	1.89	3767
24	4.82	1.08	0.1174	0.0670	1.75	3795
26	3.98	0.928	0.1134	0.0607	1.56	3778
28	3.16	0.769	0.1083	0.0524	1.33	3704
30	2.40	0.610	0.1037	0.0445	1.05	3836
32	1.70	0.461	0.0972	0.0335	0.731	3765
34	1.09	0.317	0.0906	0.0217	0.391	3550
36	0.545	0.160	0.0898	0.0202	0.034	3586

REFERENCES

1. Davidson, J. M. Thermally Induced Length Changes of Graphite Cubes, HW-65815. June 24, 1960.
2. Passel, T. O. and R. L. Heath. "Fission Neutron Cross Section Measurements for Threshold Reactions," Trans. Am. Nuclear Soc., 2, No. 2: 21-23. November, 1959.
3. Hogg, C. H. and L. D. Weber. "The Neutron Cross Section of Cobalt-58," Trans. Am. Nuclear Soc., 3, No. 2: 462. December, 1960.
4. Hogg, C. H. Personal Communications. August, 1960.
5. Bilodeau, G. G., et al. PDQ - An IBM 704 Code to Solve the Two-Dimensional Few-Group Neutron-Diffusion Equations, WAPD-TM-70. August, 1957.
6. Preskitt, C. A. Personal Communications. June, 1960.
7. Woodfield, F. W. (ed.). Unclassified Research and Development Programs Executed for the Division of Reactor Development and the Division of Research, HW-68172. January 10, 1961.
8. de Halas, D. "Nuclear Graphite," Chapter 7, edited by R. E. Nightingale. Book to be published.
9. Davidson, J. M., et al. "High Temperature Radiation Induced Contraction in Graphite," Proceedings of the Fourth Carbon Conference, Buffalo: 599-609. 1960.
10. McAdams, W. H. Heat Transmission, 3d ed., New York: McGraw-Hill, 1954.
11. Bush, P. D., et al. Engineering Test Reactor Engineering Design and Safeguards Report, IDO-24020. July, 1956.
12. Atomic Energy Commission. The Reactor Handbook, AECD-3646, AECD-3647. May, 1955.
13. American Lava Corporation. AlSiMag, Chart No. 591. Chattanooga, undated.
14. Aluminum Company of America. Alcoa Structural Handbook. Pittsburgh: Aluminum Company of America, 1956.
15. Marks, L. S. (ed.). Mechanical Engineers' Handbook, 5th ed. New York: McGraw-Hill, 1951.
16. Yoshikawa, H. H. Flux Monitoring for Radiation Damage Studies, HW-64251. March 3, 1960.

INTERNAL DISTRIBUTION

Copy Number	
1	F. W. Albaugh - H. M. Parker
2	D. E. Baker
3	R. W. Benoliel
4	J. H. Brown
5	D. H. Curtiss
6	R. E. Dahl
7 - 16	J. M. Davidson
17 - 57	D. R. deHalas
58	R. L. Dillon
59	J. E. Faulkner
60	J. F. Fletcher
61	J. C. Fox
62 - 67	J. W. Helm
68	F. D. Hobbs
69	J. L. Jackson
70	G. A. Last
71	C. E. Love
72	D. B. Lovett
73	J. E. Minor
74	W. C. Morgan - R. C. Giberson
75	I. T. Myers
76	R. Neidner
77	R. E. Nightingale
78	F. W. Woodfield
79	R. E. Woodley
80	E. M. Woodruff
81	H. H. Yoshikawa
82 - 96	Extra
97	300 Files
98	Record Center
99 - 102	G. E. Technical Data Center, Schenectady

SPECIAL EXTERNAL DISTRIBUTION

Number of Copies	
1	Argonne National Laboratory Attn: R. M. Adams
1	Brookhaven National Laboratory Attn: D. H. Gurinsky
2	Division of Reactor Development Attn: R. E. Pahler I. F. Zartman
3	General Atomic Division Attn: R. B. Duffield W. Kosiba R. A. Meyer
2	General Electric Company, Vallecitos Atomic Laboratory Attn: L. P. Bupp E. W. O'Rorke
1	General Electric Research Laboratories Attn: E. R. Stover P.O. Box 1088, Schenectady
1	General Nuclear Engineering Corporation Attn: W. A. Maxwell
1	Great Lakes Carbon Corporation Attn: L. H. Juel, Electrode Division Research and Development Department P.O. Box 637, Niagara Falls, New York
1	Hanford Operations Office
2	Attn: J. M. Musser R. L. Plum
1	National Carbon Company Attn: W. P. Eatherly, Carbon Division P.O. Box 6116, Cleveland 1, Ohio
2	Oak Ridge National Laboratory (Y-12) Attn: F. L. Carlsen R. A. Charpie
2	Oak Ridge Operations Office Attn: W. J. Larkin D. F. Cope
1	Marquardt Corporation Attn: D. W. Bareis
1	Speer Carbon Company Attn: W. E. Parker Research and Development Laboratories Packard Road & 47th Street, Niagara Falls
1	Wright Air Development Division Attn: R. H. Wilson (Capt.)

EXTERNAL DISTRIBUTION

Number of Copies	
11	Aberdeen Proving Ground
1	Aerojet-General Corporation
1	Aerojet-General Nucleonics
1	AFPR, Boeing, Seattle
2	AFPR, Lockheed, Marietta
2	Air Force Special Weapons Center
2	ANP Project Office, Convair, Fort Worth
1	Alco Products, Inc.
1	Allis-Chalmers Manufacturing Company
1	Allis-Chalmers Manufacturing Company, Washington
1	Allison Division - GMC
10	Argonne National Laboratory
1	Army Ballistic Missile Agency
3	Army Chemical Center
1	Army Chemical Center (Taras)
1	Army Chemical Corps
1	Army Medical Research Laboratory
1	Army Signal Research and Development Laboratory
1	AEC Scientific Representative, France
1	AEC Scientific Representative, Japan
3	Atomic Energy Commission, Washington
4	Atomic Energy of Canada Limited
4	Atomics International
4	Babcock and Wilcox Company
2	Battelle Memorial Institute
4	Brookhaven National Laboratory
1	Brush Beryllium Company
1	Bureau of Medicine and Surgery
1	Bureau of Mines, Albany
1	BUWEPSREP, Goodyear Aircraft, Akron
1	Bureau of Ships (Code 1500)
1	Bureau of Yards and Docks
1	Carnegie Institute of Technology
1	Chicago Operations Office
1	Chicago Patent Group
1	Combustion Engineering, Inc.
1	Combustion Engineering, Inc. (NRD)
1	Convair-General Dynamics Corporation, San Diego
3	Defence Research Member
1	Denver Research Institute
2	Department of the Army, G-2
3	duPont Company, Aiken
1	duPont Company, Wilmington
1	Edgerton, Germeshausen and Grier, Inc., Goleta

EXTERNAL DISTRIBUTION (contd.)

Number of Copies

3	Pratt and Whitney Aircraft Division
1	Princeton University (White)
2	Public Health Service
1	Public Health Service, Las Vegas
1	Public Health Service, Montgomery
1	Quartermaster Food and Container Institute
1	Quartermaster Research and Development Command
1	Radiation Applications, Inc.
1	Rensselaer Polytechnic Institute
3	Sandia Corporation, Albuquerque
1	Strategic Air Command
1	Sylvania Electric Products, Inc.
1	Technical Research Group
1	Tennessee Valley Authority
2	Union Carbide Nuclear Company (ORGDP)
6	Union Carbide Nuclear Company (ORNL)
1	USAF Project RAND
1	U. S. Geological Survey, Denver
1	U. S. Geological Survey, Naval Gun Factory
1	U. S. Geological Survey, Washington
1	U. S. Naval Ordnance Laboratory
1	U. S. Naval Postgraduate School
2	U. S. Naval Radiological Defense Laboratory
1	U. S. Patent Office
2	University of California, Berkeley
2	University of California, Livermore
1	University of Puerto Rico
1	University of Rochester
1	University of Rochester (Marshak)
1	Watertown Arsenal
4	Westinghouse Bettis Atomic Power Laboratory
1	Westinghouse Electric Corporation
7	Wright Air Development Division
1	Yankee Atomic Electric Company
325	Office of Technical Information Extension
75	Office of Technical Services, Washington